AD-A106 790 HUGHES RESEARCH LABS MALIBU CA F/G 7/4
ESTER LIQUID CRYSTAL MIXTURES FOR DYNAMIC SCATTERING AT ELEVATE--ETC(U)
OCT 81 J D MARGERUM, A M LACKNER N00014-79-C-524
UNCLASSIFIED TR-2 NL

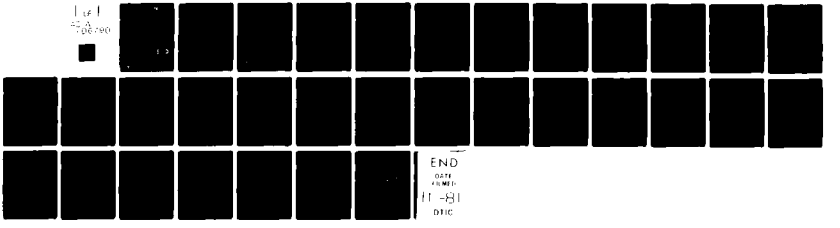

END
DATE FILMED
11-81
DTIC

(12) LEVEL II

AD A106790

OFFICE OF NAVAL RESEARCH

Contract N00014-79-C-0524

TECHNICAL REPORT NO. 2

ESTER LIQUID CRYSTAL MIXTURES FOR DYNAMIC SCATTERING AT ELEVATED TEMPERATURES

by

J. David Margerum and Anna M. Lackner

Accepted for Publication in

Molecular Crystals and Liquid Crystals

Hughes Research Laboratories
3011 Malibu Canyon Road
Malibu, California 90265

DTIC
ELECTE
S NOV 3 1981 D
B

OCTOBER 1981

DTIC FILE COPY

Reproduction in whole or in part is permitted for any purpose of the United States Government

Approved for Public Release; Distribution Unlimited

8 1 11 02 230

UNCLASSIFIED

SECURITY CLASSIFICATION OF THIS PAGE (When Data Entered)

REPORT DOCUMENTATION PAGE		READ INSTRUCTIONS BEFORE COMPLETING FORM
1. REPORT NUMBER Technical Report No. 2	2. GOVT ACCESSION NO. AD-A106 780	3. RECIPIENT'S CATALOG NUMBER
4. TITLE (and Subtitle) ESTER LIQUID CRYSTAL MIXTURES FOR DYNAMIC SCATTERING AT ELEVATED TEMPERATURES.		5. TYPE OF REPORT & PERIOD COVERED Technical 6. PERFORMING ORG. REPORT NUMBER
7. AUTHOR(s) J. David Margerum and Anna M. Lackner		8. CONTRACT OR GRANT NUMBER(s) N00014-79-C-0524
9. PERFORMING ORGANIZATION NAME AND ADDRESS Hughes Research Laboratories 3011 Malibu Canyon Road Malibu, CA 90265		10. PROGRAM ELEMENT, PROJECT, TASK AREA & WORK UNIT NUMBERS NR 372
11. CONTROLLING OFFICE NAME AND ADDRESS Office of Naval Research/Chemistry Program Code 472 Arlington, VA 22217		12. REPORT DATE October 1981 13. NUMBER OF PAGES 30
14. MONITORING AGENCY NAME & ADDRESS(if different from Controlling Office)		15. SECURITY CLASS. (of this report) UNCLASSIFIED 15a. DECLASSIFICATION/DOWNGRADING SCHEDULE

16. DISTRIBUTION STATEMENT (of this Report)

Approved for public release; distribution unlimited

17. DISTRIBUTION STATEMENT (of the abstract entered in Block 20, if different from Report)

18. SUPPLEMENTARY NOTES

Accepted for publication in Molecular Crystals and Liquid Crystals

19. KEY WORDS (Continue on reverse side if necessary and identify by block number)

Nematic liquid crystals
DC-activated dynamic scattering
Flat panel matrix displays
Ester liquid crystal mixtures
Elevated temperature effects

20. ABSTRACT (Continue on reverse side if necessary and identify by block number)

Studies are made on the effect of elevated temperature on the properties, thermal stability, and dynamic scattering (DS) of liquid crystal, ester mixtures. Six eutectic nematic mixtures are formulated with clearpoints in the range of 72° to 81°C; structural effects are evaluated by using different combinations of components from eight classes of esters, including phenyl benzoates, phenyl thiobenzoates, phenyl cyclohexanecarboxylates, phenyl acloxybenzoates, as well as a phenyl benzoyloxybenzoate and a phenyl

DD FORM 1 JAN 73 1473

UNCLASSIFIED

SECURITY CLASSIFICATION OF THIS PAGE (When Data Entered)

biphenylcarboxylate structure. The mixtures are characterized at 25°C, and their viscosity, dielectric anisotropy, conductivity anisotropy, and dc-activated DS effects are studied as a function of temperature. Thermal instabilities are studied at 100°C, with and without redox conductivity dopants. The DS stability with 20 V dc is studied at 55°C for three of the more stable mixtures, both in transparent cells and in cells with reflective metal electrodes.

Accession For	
NTIS GRA&I	☑
DTIC TAB	☐
Unannounced	☐
Justification	
By	
Distribution/	
Availability Codes	
Dist	Avail and/or Special
A	

ESTER LIQUID CRYSTAL MIXTURES FOR DYNAMIC SCATTERING AT ELEVATED TEMPERATURES

J. David Margerum and Anna M. Lackner

Hughes Research Laboratories

3011 Malibu Canyon Road

Malibu, California 90265

ABSTRACT

Studies are made on the effect of elevated temperature on the properties, thermal stability, and dynamic scattering (DS) of liquid crystal, ester mixtures. Six eutectic nematic mixtures are formulated with clearpoints in the range of 72° to 81°C; structural effects are evaluated by using different combinations of components from eight classes of esters, including phenyl benzoates, phenyl thiobenzoates, phenyl cyclohexanecarboxylates, phenyl acyloxybenzoates, as well as a phenyl benzoyloxybenzoate and a phenyl biphenylcarboxylate structure. The mixtures are characterized at 25°C, and their viscosity, dielectric anisotropy, conductivity anisotropy, and dc-activated DS effects are studied as a function of temperature. Thermal instabilities are studied at 100°C, with and without redox conductivity dopants. The DS stability with 20 V dc is studied at 55°C for three of the more stable mixtures, both in transparent cells and in cells with reflective metal electrodes.

INTRODUCTION

The dynamic scattering (DS) mode[1] is being studied for liquid crystal (LC) applications such as flat-panel pictorial matrix displays,[2-4] programmable reticle devices,[5,6] and automobile dashboard displays.[7] These devices need to be capable of both storage and operation over a wide range of ambient temperatures, particularly when used for military applications or in automobiles. For example, storage temperatures from -60° to 80°C and ambient operating temperatures of -50° to 71°C are typical requirement goals for these devices. Also, the pictorial matrix displays have been developed using circuits in which the LC is activated by direct current (dc) signals. However, there is a dearth of information on the characteristics and stability of dc-DS in LCs at various temperatures. The present study has been initiated to evaluate these issues. Since it is relatively simple to quickly heat the thin LC layer in many devices, we emphasize here studies on the effects of elevated temperatures on the LC. Previous results[8,9] in our laboratory showed that long-period dc-DS stability was obtained at room temperature by using specially selected dopants in phenyl benzoate LC mixtures. Thus, we have chosed to study the redox dopant pair consisting of dibutylferrocene (DBF) and 2,4,7-trinitro-9-fluorenylidenemalononitrile (TFM) in various ester LC mixtures. Different combinations of components from the eight classes of ester LCs shown in Figure 1 are used in six new mixtures as a means of evaluating structural effects on DS and thermal stability.

EXPERIMENTAL

The RO-R', RO-OR', ROSR' components are prepared by standard esterification techniques using intermediates commercially obtainable from Eastman Kodak or Aldrich Chemical. The ester synthesis, purification, and analysis techniques are carried out in the manner recently described for the RO-R' components.[10] The RO-[C]R' components are prepared as described recently.[11] The RO-OOCR' components are synthesized by first preparing the appropriate 4-acyloxybenzoyl chloride and then reacting it with an alkoxyphenol to obtain the RO-OOCR' acyloxy ester. These are purified by preparative liquid chromatography (using Waters Association's System 500 instrument) as well as by recrystallizations. The R-(Cl)OOCϕR' component is purchased from Eastman Kodak (EK 11650) and is recrystallized before use. The R(CN)-ϕR' component is purchased from E. Merck (S-1014 Licristal) and is used as received. Thin-layer chromatography and liquid chromatography analyses indicate that the impurity content is less than 0.5% for each of the components. The redox dopants (DBF and TFM) were obtained commercially and were purified as in previous studies.[9]

The thermal analysis by differential scanning calorimetry (DSC), the molecular length (L), flow viscosity (η), birefringence (Δn), dielectric anisotropy ($\Delta\varepsilon$), resistivity (ρ), conductivity anisotropy ($\sigma_{\parallel}/\sigma_{\perp}$), and the DS voltage thresholds, scattering curves, and response times are measured by techniques recently described.[10,11] Low temperature stability is measured by cooling LC samples in capped test tubes for extended periods (more than a month) at -40°C, then transferring the tubes to a controlled isopropanol bath at -20°C and observing the temperature at which all of the crystals melt as the bath is gradually warmed. The DS response times are measured using the LC between optical flats with SiO_x pad spacers of 8.4 μm thickness, using surface-parallel alignment obtained by rubbing polyvinyl alchohol (PVA) coatings. The PVA, which is oven-baked after being spin-coated from aqueous solution, is

estimated to be about 500 Å thick. The unsealed cells in the 100°C thermal stability tests have float glass (FG) substrates coated with an indium tin oxide (ITO) transparent conductor. These are thoroughly cleaned, are ion-beam etched (IBE) for surface-∥ alignment,[12] and are used with 13 μm Mylar spacers. The sealed test cells have FG/ITO/PVA substrates, are sealed using an epoxy coated Mylar film (Ablefilm 539, Type II) of 13 μm thickness, and are back filled with LC after evacuation. Both the unsealed and the sealed cells used in the tests of electrochemical stability at 55°C have FG/ITO/PVA substrates.

RESULTS AND DISCUSSION

LC Components and Mixtures

The estimated molecular length and the thermal properties of components used in the mixtures are shown in Table I. The melting points and the heats of fusion are used with the Schroeder-Van Laar equation to calculate the eutectic compositions of the mixtures shown in Table II, with the exception of HRL-256N5, which is a eutectic mixture that is experimentally determined. All of the mixtures contain RO-R' and RO-OR' components, but vary in their content of other components. The HRL-2N52 mixture has only RO-OOCR' acyloxy compounds added; HRL-25N4 has only thioesters added; HRL-26N3 has only RO-[C]R' components and the R-(Cl)OOCϕR' diester added; HRL-26N4 has only acyloxy and RO[C]R' components added; HRL-246N1 has only RO-[C]R' and the R(CN)-ϕR' biphenyl ester added; while HRL-265N5 has thioesters, acyloxy esters, and a RO-[C]R' ester added. A unique feature of these eutectic mixtures is the inclusion of binary sets of components, which have essentially the same molecular length, but are from different classes of esters. Such binary eutectic components are 60-01 and 10S06 in HRL-25N4 and HRL-256N5; and 20-3 and 20-[C]3 in HRL-26N4 and HRL-256N5. Similarly, 60-5, 60-[C]5,

and 80-3 are combined as a tertiary mixture of this type used in HRL-26N3. The use of such binary sets is of particular value in preparing eutectic mixtures with relatively short molecular length components.

The components are chosed to give a clearpoint above 71°C and a wide nematic range, as shown by the calculated melting points and clearpoints in Table III. The observed clearpoints (which are at the low end of the clearpoint range) are about 1° to 3° lower than the calculated values. The melting points are difficult to determine because all of the mixtures tend to supercool. The observed melting points in Table III are recorded as the temperature at which the last crystals melt in a bulk sample of the mixture after an extended period at -40°C. After cooling, the HRL-26N4 and HRL-246N1 mixtures contain small amounts of crystalline material that melt near room temperature; the calculated eutectic compositions are probably somewhat different from the actual eutectics obtainable with the same components. The HRL-26N3 mixture gives the best low temperature eutectic properties, possibly because it contains neither acyloxy nor biphenyl esters.

Room-Temperature Properties

The calculated average molecular length of the mixtures and several of their room-temperature anisotropic properties are also shown in Table III. The birefringence of the mixtures is increased by thioester components and is decreased substantially by the RO-[C]R' cyclohexanecarboxylate components. The viscosity is strongly increased by the R(CN)-ϕR' component and is greatly decreased by the RO-[C]R' component. Other studies[13] in our laboratory indicate that the η contribution of the components decreases in the following sequence: R(CN)-ϕR' > R-(Cl)OOCϕR' > ROSOR' > RO-OR' > RO-OOCR' > ROSR' > RO-R' > RO-[C]R'. The dielectric anisotropy of the mixtures is most affected by the strongly negative o-cyano R(CN)-ϕR' component, by the negative

RO-[C]R' components, and by the strongly positive R-(Cl)OOCϕR' component; we estimate the $\Delta\varepsilon$ of these ester classes to be approximately -3.7, -1.3, and 5.5, respectively. The conductivity anisotropy of the redox dopant is approximately the same in four of the mixtures, but is distinctly lower in the HRL-2N52 and HRL-26N3 mixtures.

The DS threshold voltages (V_{th}) for these redox-doped mixtures are summarized in Figure 2, which shows the effect of surface alignment, $\Delta\varepsilon$, and the use of ac and dc voltages. The effect of $\Delta\varepsilon$ on the ac thresholds (both surface-$\parallel$ and surface-$\perp$) is similar to that reported[14] for other LC mixtures. The same type of effect is seen here for the dc-V_{th}, which are at lower voltages, although the dc-V_{th} values are less reproducible than the ac-V_{th} values. The general effect of $\Delta\varepsilon$ on V_{th} is observed despite the compositional differences in these ester mixtures, probably because all of the mixtures are esters with some common components and similar $\sigma_{\parallel}/\sigma_{\perp}$ values, as well as similar clearpoints. The mixtures with the best dc-V_{th} values are HRL-25N4 and HRL-256N5, each of which contains thioester components.

The dc-DS curves of scattering (where % S= 100 - % T) versus voltage are shown in Figure 3 for the six mixtures in surface-$\parallel$ cells. A gradual increase in the scattering levels between their V_{th} and about 10 to 12 V is considered a favorable feature for achieving a gray scale capability in pictorial matrix displays. The DS response times generally increase as the viscosity of the mixtures increase, as shown in Figure 4 where the on-time is the sum of the delay time and the rise time. The mixtures with the fastest response times are those with the lowest viscosities, namely HRL-26N3 and HRL-24N4.

Properties at Elevated Temperatures

The effects of elevated temperatures are determined for several anisotropic properties of these mixtures. The flow viscosities in the

25°to 65°C range are shown in Figure 5. They all follow similar patterns and have relatively larger η values at the lower temperatures than would be expected from a linear plot of log η versus T^{-1}. This may be related to some cybotactic nematic characteristics, as discussed below. The temperature dependence of $\Delta\varepsilon$ and $\varepsilon_\perp$ is shown in Figures 6 and 7. The only unusual effect is that the $\Delta\varepsilon$ of HRL-26N3 changes from slightly positive at room temperature to slightly negative between 50°C and its clearpoint. Three of the mixtures (HRL-2N52,-25N4, and -26N3) show relatively small changes in their $\Delta\varepsilon$ values between 20° and 60°C. The effect of temperature on $\sigma_\parallel/\sigma_\perp$ is shown in Figure 8. As mentioned above, four of the mixtures have fairly high $\sigma_\parallel/\sigma_\perp$ values of 1.40 to 1.45 at 25°C while HRL-26N3 and HRL-2N52 have smaller conductivity anisotropies. The latter two mixtures also show the most evidence of cybotactic nematic character[15] (short-range smectic order) at lower temperatures, as indicated by the increase of $\sigma_\parallel/\sigma_\perp$ with increasing temperature to give a maximum $\sigma_\parallel/\sigma_\perp$ value.[16] The cybotactic nematic effects cause lower $\sigma_\parallel/\sigma_\perp$ values in HRL-26N3, and are responsible for its relatively higher V_{th} values in surface-$\parallel$ cells at 23°C (Figure 2). The effect of temperature on resistivity is shown in Figure 9, where the spread of $\rho_\perp$ values at a given temperature is caused by differences in the concentration of ions produced by the redox dopants in these LC mixtures. In these plots, the temperature effects on $\rho_\perp$ are roughly parallel for all of the mixtures except HRL-26N3. Its slightly smaller slope is probably related to its strong cybotactic nematic characteristics. In general, $\rho_\perp$ changes by an order of magnitude in the 45° range, between 25° and 70°C. Slightly steeper plots of this type are obtained for the apparent dc-resistivity of these mixtures in surface-$\parallel$ cells when DS is activated with 20 Vdc. In the latter case, the apparent ρ_{dc} changes by an order of magnitude in the 36° range, between 35° and 71°C. This latter range corresponds to the practical temperature range of operating a pictorial matrix display cell if the ρ_{dc} of the LC in it has to be maintained between 10^9 and 10^{10} Ω-cm.

This is the approximate ρ_{dc} range required in a matrix display, so that at 71°C the charge on each pixel capacitor does not leak off too fast in 1/30 a sec frame time (i.e. $\rho_{dc} > 10^9 \Omega$-cm). And, so that at 35°C, the LC is conductive enough to show good DS (i.e., $\rho < 10^{10}$ Ω-cm).

Dynamic Scattering at Elevated Temperatures

The dc-DS curves of scattering versus voltage have several characteristic changes at elevated temperature, but as shown in Figures 10 and 11, the effects are not large. In general the dc-V_{th} decreases as the temperature increases; and at higher temperatures the scattering levels are relatively better in the voltage range below 10 V, and poorer in the voltage range above 10 V. The temperature effects on DS do not appear to be strongly affected by $\Delta\varepsilon$ changes, since the $\Delta\varepsilon$ of HRL-26N3 changes from about 0.07 to -0.01 in the temperature range in Figure 10, while the $\Delta\varepsilon$ for HRL-26N4 changes from about -1.0 to -0.7 in the similar results shown in Figure 11.

The DS response times are more strongly affected by temperature, as shown in Figure 12 for the three more stable mixtures. The data are presented as log τ versus T^{-1} to permit comparisons with similar plots of the viscosity (Figure 5) and resistivity (Figure 9) changes with temperature. In the lower temperature range the τ_D and τ_{ON} decrease with increasing temperature in the same manner as η decreases. But in the upper temperature range, the response times tend to level off and change less with temperature. Nevertheless, the response times are generally faster at higher temperatures, where they are more suitable for displaying TV rate pictures with LC devices. In a TV rate matrix display, it is particularly advantageous to have $\tau_{ON} <$ frame time $\leq \tau_D$, and to have a high τ_D/τ_{ON} ratio at elevated temperatures, where the activating voltage from a pixel capacitor may decrease during the frame time as a result of the increased conductivity of the LC. The HRL-2N52 mixture in Figure 12 shows such a favorable condition at 64°C

with τ_{ON} = 7 ms and τ_D = 70 ms, that in a 33.3 ms frame time it reaches nearly full DS in about 1/5 of the frame, and decays fully in a little more than two frames.

Thermal Stability at Elevated Temperatures

Many of our thermal stability tests are summarized in Table IV, which shows results from heating samples at an accelerated temperature of 100°C. Four of the mixtures showed excellent stability when heated as bulk samples in evacuated glass test tubes for 2,500 h at 100°C, after first degassing them on a vacuum line with a freeze/thaw technique. The other two mixtures (HRL-25N4 and HRL-246N1) showed no significant change in clearpoint, but showed a small increase in conductivity, and slight yellow coloration in the evacuated tubes. Relatively good stability was shown by all of the mixtures after heating for 3,200 h at 100°C in crimp-sealed Al DSC pans. There was no change in clearpoint. but after removal from the pans, the samples showed substantial decreases in resistivity, and the conductive species produced dc-DS in four of the mixtures. This indicates probable thermal sensitivity to oxygen, since the DSC pans were not evacuated. The decreased resistivity is a serious problem if the ionic species thus generated interfere with the electrochemical reversibility of the LCs when redox dopants are present. Poor stability was found when heating the mixtures (1,980 h at 100°C) as thin LC layers (13 μm thick) in unsealed test cells with FG/ITO/IBE glass substrates. Even though heated in a N_2-flushed oven, all of the unsealed cells showed decomposition in the form of some high melting crystalline products in the LCs. The crystals must be reaction products because their melting points are higher than those of any of the initial components. Some of the products may be LCs since the clearpoint of the remaining LC fluid is increased in each mixture. However, because of the small quantity of the products and the complexity of the initial multicomponent mixtures, we have not yet identified the products.

No crystal formation is observed in the thin-layer test cells that are evacuated and sealed. As indicated in Table IV, three of the mixtures were heated for 2,820 h at 100°C. However, contaminates from the epoxy sealant causes the resistivity of the LCs to decrease substantially. These ionic impurities do not provide good electrochemical stability to the LC, as found by rapid degradation of the undoped LC in the sealed cells at 20 Vdc and 55°C after their long period of heating at 100°C. Other qualitative tests show that crystalline products are not formed in heated evacuated tubes with water added, but that they are formed rapidly in unsealed cells made up on glass substrates (no ITO) heated at 100°C in a N_2-flushed oven. Bulk samples heated in air do not produce products as rapidly as thin cells with glass substrates. Thus the main thermal instability observed for the undoped LCs appears to result from the presence of both glass surfaces and oxygen.

Studies of the thermal stability of the LC mixtures with redox dopants (DBF and TFM) added are also shown in Table IV. Evacuated tubes containing 1% of the redox dopants were heated for 2,300 h at 100°C. The results indicate that the mixtures with fairly good thermal stability with the redox dopants are HRL-26N3,-26N4, and-2N52. (The stability of HRL-2N52 is implied on the basis of common components with the others, and this has been confirmed by other tests described below.) The HRL-25N4 mixture contains the most thioester components and reacts most rapidly with the redox dopants at 100°C. The HRL-256N5 also contains a thioester and shows some reaction. The reactivity of the HRL-246N1 mixture with the redox dopant is believed to be caused by its biphenyl component, which is the only ester class in HRL-246N1 that is not in HRL-26N3 and -26N4. A well-sealed test cell (FG/ITO/PVA substrates sealed with Type II Abelfilm 539, and evacuated) containing a layer of HRL-2N52 13 μm thick with 0.25% redox dopant, showed no crystals or discoloration after 5,430 h of heating at 100°C. Collectively, these results indicate that five of the eight classes of LC esters in Figure 1 have good thermal stability, even in the presence of the redox dopant.

Electrochemical Stability at Elevated Temperatures

Although we have successfully operated redox-doped LC sealed cells (made with Ablefilm 539) for long periods at 20 Vdc at room temperature, we find that they can be operated for only a few days at 55°C before deposits appear on the ITO electrodes. As mentioned above, this problem arises because the sealant introduces ionic impurities that cause electrochemical degradation even in undoped LCs. Thus, we have tested the electrochemical stability of unsealed cells at 55°C in a N_2-flushed oven, even though we know that some thermal instability can be expected to occur gradually in these unsealed cells. Typical results are shown in Figure 13 for our three most thermally stable LC/redox mixtures, with a range of DBF/TFM concentrations, and with reflective as well as transmission-type cells. No serious defects appeared in any of the cells until after 1,500 h at 20 Vdc and 55°C. More stable resistivity values are observed in the two cells with reflective Ag electrodes, one of which contained HRL-2N52, and the other HRL-26N4. In general, the electrochemical stability of the three more thermally stable mixtures with redox dopants appears to be fairly good at 55°C, and probably would be much better in evacuated cells made with a non-contaminating sealant.

CONCLUSIONS

Wide-temperature nematic eutectic mixtures can be made using multiple components from several classes of ester structures, including esters of essentially the same molecular length from different classes. In general, low V_{th} for DS occurs with high $\sigma_{\parallel}/\sigma_{\perp}$ and small $\Delta\varepsilon$ values (in surface-$\parallel$ cells), and fast response is favored by low η. Among the eight ester classes studied in six mixtures, the RO-[C]R', RO-R', and ROSR' structures have relatively low η while the R(CN)-ϕR' and R-(Cl)OOCϕR' structures have relatively high η. Good thermal stability

at 100°C, in the presence of the DBF/TFM redox dopants, is shown in evacuated tubes for three mixtures which include five different classes of esters. Structures having lower stability with redox dopants are the thioesters and a biphenylcarboxylate ester. One of our thermally stable mixtures, HRL-26N3, has the widest nematic range (-20° to 76°) as well as the lowest η and the fastest dc-DS response times of the six mixtures; however, it shows cybotactic nematic characteristics, and has lower $\sigma_{\parallel}/\sigma_{\perp}$ valued than most of the other mixtures. The temperature dependence of ρ_{dc} changes approximately on an order of magnitude between 35° and 71°C. Some of the dc-DS characteristics improve at elevated temperatures, notably the V_{th} decreases, and the τ_{ON} becomes short compared to the typical 33 ms frame-time of a matrix display. Relatively good dc-DS operating lifetime is demonstrated at elevated temperatures (>1,500 h at 20 Vdc and 55°C) in unsealed cells, However, accelerated tests at 100°C show that the LCs in unsealed test cells are thermally decomposed by traces of oxygen, and that this instability is catalyzed by glass surfaces. This thermal decomposition is avoided in evacuated cells made with an epoxy film sealant. However, elevated temperatures generate conductivity impurities in the LC from epoxy sealants. These impurities greatly reduce the dc-DS lifetime of the redox-doped mixtures at elevated temperatures, indicating that improved sealants are needed.

ACKNOWLEDGEMENTS

This work was supported in part by the Office of Naval Research. We are indebted to S.-M. Wong and C.I. van Ast for assistance in synthesis and in viscosity measurements; to W.H. Smith, Jr., for assistance in the DSC measurements; and to G.D. Myer and J.E. Jensen for assistance in the characterization of the mixtures.

References

1. F.G. Heilmeier, L.A. Zanoni, and L.A. Barton, Proc. IEEE 56, 1162 (1968).
2. M.H. Ernstoff, A.M. Leupp, M.J. Little, and H.T. Peterson, IEEE Electron Device Conf. Digest, Washington, D.C. (Dec. 1973).
3. J.D. Margerum and L.J. Miller, J. Colloid and Interface Sci. 58, 559 (1977).
4. M. Yoshiyama, T. Matsuo, K. Kawasaki, H. Tatsuta, and T. Ishihara, 8th Int'l Liq. Cryst. Conf. paper I-14, Kyoto, Japan (July 1980).
5. C.H. Gooch, R. Bottomley, J.J. Low, and H.A. Tarry, J. Phys, E 6, 485 (1973).
6. R.P. Farnsworth, L.W. Hill, and S.-Y. Wong, U.S. Patent 3,885,861 (May 27, 1975).
7. Y. Ohsawa, T. Fujii, Y. Okada, and S. Kanabe, 8th Int'l Liq. Cryst. Conf., Paper I-26P, Kyoto, Japan (July 1980).
8. H.S. Lim and J.D. Margerum, Appl. Phys. Lett., 28, 478 (1976).
9. H.S. Lim, J.D. Margerum, and A. Graube, J. Electrochem. Soc. 124, 1389 (1977).
10. J.D. Margerum, J.E. Jensen, and A.M. Lackner, Mol. Cryst. Liq. Crys. (in press, 1981).
11. J.D. Margerum, S.-M. Wong, A.M. Lackner, and J.E. Jensen, Mol. Cryst. Liq. Cryst. (in press, 1981).
12. M.J. Little, H.L. Garvin, and L. J. Miller, Liquid Crystals and Ordered Fluids, J.E. Johnson and R.S. Porter, Eds. (Plenum Press 1978), 3, p. 497.
13. J.D. Margerum, Anisotropic and Electro-Optical Effects in Liquid Crystals, AFOSR Contract N49620-77-C-0017 Final Report (April 1981).
14. M.I. Barnik, L.M. Blinov, M.F. Grebenkin, S.A. Pikin, and V.G. Chigrirov, Sov. Phys. JETP 42, 550 (1976).
15. A. DeVries, J. de Physique (Paris) Colloq. C136, 1 (1975).
16. G. Heppke, and F. Schneider, Z Naturforsch 30a, 316 (1975).

Table I. Thermal Properties of Components

Class Code	Compound Code[a]	Molecular Length,[b] (Å)	Melting Point, °C	Clear-point °C	ΔH_f, Kcal/Mole
RO-R'	20-3	19.67	75.4	65.2	6.26
RO-R'	20-5	22.21	62.8	63.4	7.04
RO-R'	40-6	25.81	39.5	48.2	7.82
RO-R'	60-5	27.03	40.9	59.3	5.54
RO-R'	80-3	26.84	51.8	56.8	6.12
RO-OR'	40-05	26.03	68.6	83.4	5.49
RO-OR'	60-01	23.60	54.9	80.4	6.19
ROSR'	10S5	21.43	63.8	70.6	5.26
ROSOR'	10S04	21.20	74.1	106.9	7.16
ROSOR'	10S06	23.90	65.0	100.1	6.47
RO-OOCR'	10-00C3	20.06	81.0	85.3	7.52
RO-OOCR'	40-00C4	25.40	67.2	83.6	8.19
RO-OOCR'	60-00C5	28.92	50.7	85.6	6.13
RO-[C]R'	20-[C]3	20.21	48.1	78.7	6.48
RO-[C]R'	40-[C]4	23.84	38.4	63.2	3.81
RO-[C]R'	60-[C]5	27.41	30.6	79.8	5.71
R-(Cl)OOCφR'	5-(Cl)OOCφ5	31.03	40.1	122.0	5.15
R(CN)-φR'	7-(CN)-φ5	29.72	44.4	103.2	5.23

[a]Where 20-3 refers to p-ethoxyphenyl p-propylbenzoate, etc.

[b]From CPK models of fully extended configurations; see references 10 and 11.

Table II. Composition of Liquid-Crystal Mixtures

Component	Mole Fraction of Component in Mixture[a]					
	2N52	25N4	26N3	26N4	246N1	256N5
20-3	0.093	0.079	0.033	0.108	0.087	0.073
20-5	0.102	0.085	—	0.120	0.094	0.076
40-6	0.189	—	—	—	—	—
60-5	—	0.256	0.147	—	—	—
80-3	—	—	0.086	—	—	—
40-05	0.147	0.127	—	—	—	0.128
60-01	0.168	0.143	0.065	0.194	0.157	0.135
10S5	—	0.155	—	—	—	0.142
10S04	—	0.057	—	—	—	—
10S06	—	0.098	—	—	—	0.094
10-00C3	0.049	—	—	0.058	—	0.041
40-00C4	0.060	—	—	0.073	—	0.049
60-00C5	0.193	—	—	0.223	—	0.120
20-[C]3	—	—	—	0.222	—	0.142
40-[C]4	—	—	0.280	—	—	—
60-[C]5	—	—	0.220	—	0.390	—
5-(C1)OOCφ5	—	—	0.169	—	—	—
7(CN)-φ5	—	—	—	—	0.272	—

[a]Calculated eutectic mixtures, except HRL-256N5, which is determined experimentally.

Table III. Properties of LC Mixtures

Property	Mixture HRL Number					
	2N52	25N4	26N3	26N4	246N1	256N5
Calculated Melting Point, °C[a]	3.0	-0.9	-15.0	6.7	1.3	-
Observed Melting Point, °C[b]	7.0	5.0	-20.0	21.0	19.0	-9.0
Calculated Clearpoint, °C[a]	73.0	74.7	77.5	78.0	83.4	-
Observed Clearpoint, °C	71.9	71.6	75.8	77.0	81.0	77.4
Average Length, Å	24.90	23.92	26.41	23.29	26.28	23.32
Δn at 23°C	0.150	0.169	0.118	0.141	0.143	0.158
η, at 25°C, cP	64.2	59.2	47.8	49.3	66.6	58.2
$\Delta\varepsilon$ at 25°C[c]	-0.48	-0.13	0.07	-0.96	-1.55	-0.51
$\sigma_{\parallel}/\sigma_{\perp}$ (Redox) at 25°C[d]	1.28	1.45	1.33	1.40	1.42	1.44

[a]For calculated eutectic mixture.

[b]Approximate temperature at which all crystals melted.

[c]Measured at 5 kHz.

[d]Measured at 100 Hz.

Table IV Thermal Stability Tests

Conditions and Measurements[a]	HRL Mixtures and Results					
	2N52	25N4	26N3	26N4	246N1	256N5
Undoped						
Initial (no heating)						
Clearpoint	71.5°	71.6°	75.9°	76.3°	80.7°	77.4°
$\rho \times 10^{-10}$	19.9	10.8	10.6	12.3	254	17.6
2,500 h at 100°C, Evacuated tubes[b]						
Clearpoint[c]	71.7°	72.0°	75.9°	76.2°	80.8°	77.2°
$\rho \times 10^{-10}$	15.6	5.63	9.44	16.3	2.41	14.5
Visual Change	none	yellow	none	none	yellow	none
3,200 h at 100°C, DSC pans[d]						
Clearpoint[c]	69.9°	70.1°	75.3°	75.1°	78.8°	76.8°
$\rho \times 10^{-10}$	0.40	0.35	0.31	0.29	0.31	0.26
DS at 20V dc	yes	yes	no	no	yes	yes
1,980 h at 100°C, unsealed cells (N_2)[e]						
Clearpoint (LC part only)	74.3°	72.2°	80.1°	81.4°	84.1°	80.6°
Melting Points of crystals in LC	112°to 133°	100°to 134°	137°to 173°	103°to 159°	115°to 169°	81°to 176°
$\rho \times 10^{-10}$	0.33	2.18	0.70	0.42	0.85	0.52
2,820 h at 100°C, sealed cells[f]						
$\rho \times 10^{-10}$	-	0.35	0.28	-	0.38	-
Crystals	-	none	none	-	none	-
1% Redox Doped						
Initial (no heating)						
Clearpoint	-	67.5°	72.0°	71.7°	76.7°	72.5°
$\rho \times 10^{-8}$	-	17.7	29.0	6.81	17.5	20.0
2,300 h at 100°C, Evacuated tubes[b]						
Clearpoint	-	67.1°	72.1°	71.6°	76.4°	72.7°
$\rho \times 10^{-8}$	-	6.22	8.98	5.43	5.52	3.71
Visual Change	-	Dark ppt.	none	none	Dark color	Dark color

[a] Temperature in °C, ρ in Ω-cm at 100 Hz and 23° in surface -# cell.

[b] Pyrex tubes.

[c] No crystals observed.

[d] Crimp-sealed Al pans.

[e] N_2-flushed oven. Cells are FG/ITO/IBE.

[f] Sealed with Ablefilm 539, Type II. Cells are FG/ITO/PVA.

10694-1

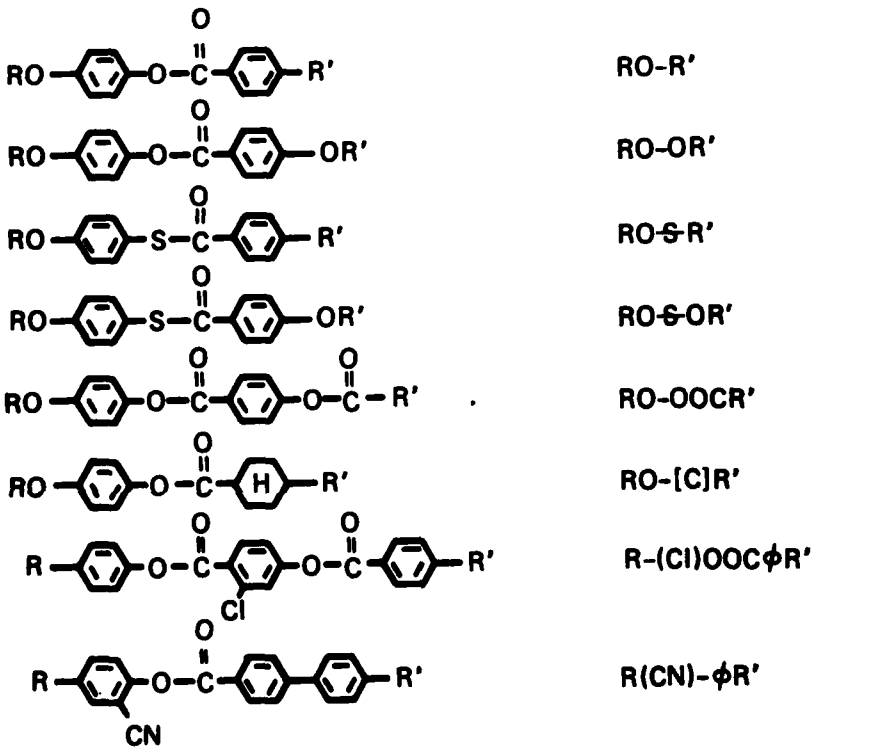

Figure 1. Structure and code symbols for the classes of LC ester components studied in mixtures.

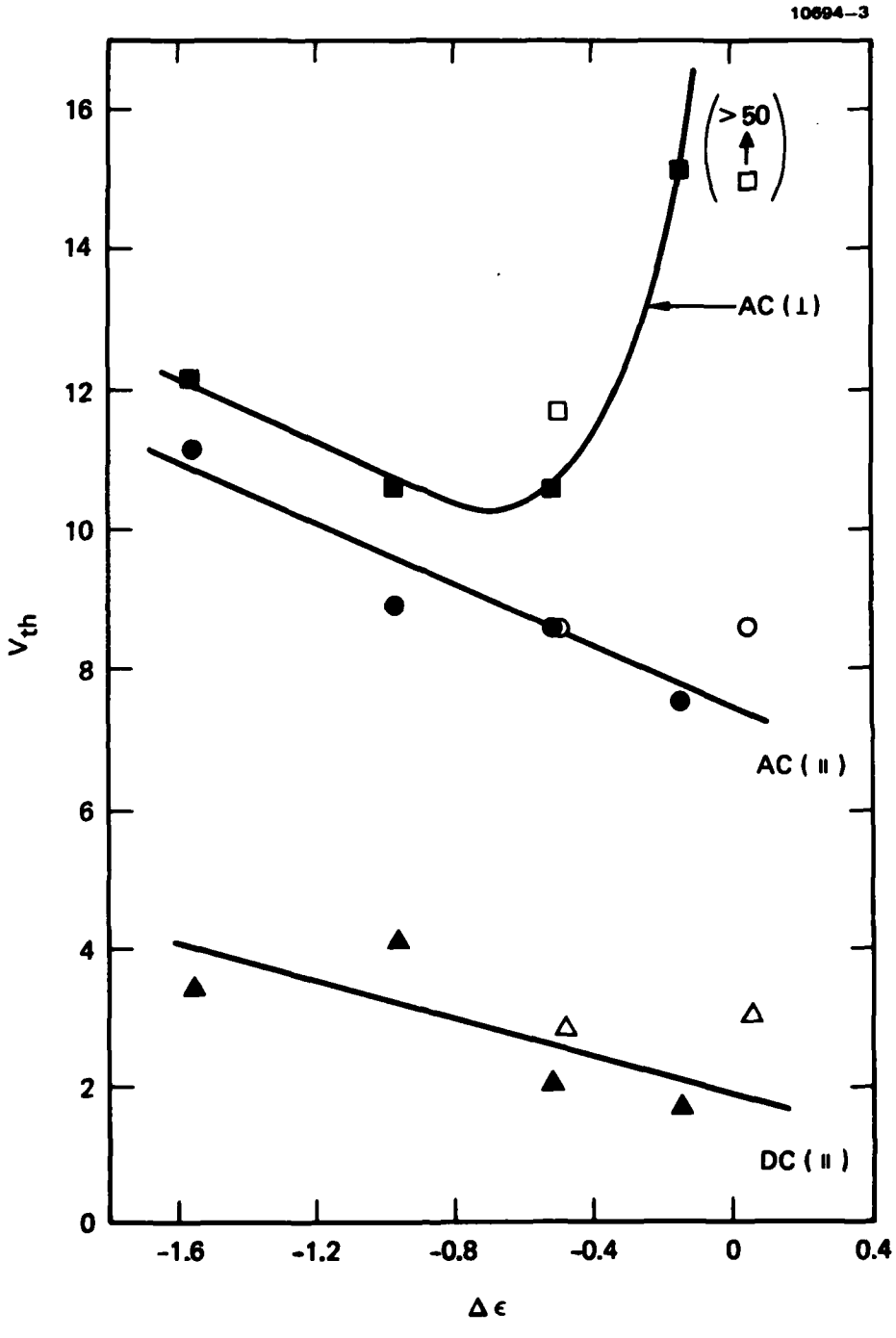

Figure 2. Effect of parameters on DS-V_{th} of redox-doped mixtures. (Transmission cells, 13 μm thick, 23°C, 0.5% DBF/TFM. Dark points have $\sigma_{\parallel}/\sigma_{\perp}$ in 1.40 to 1.45 range.)

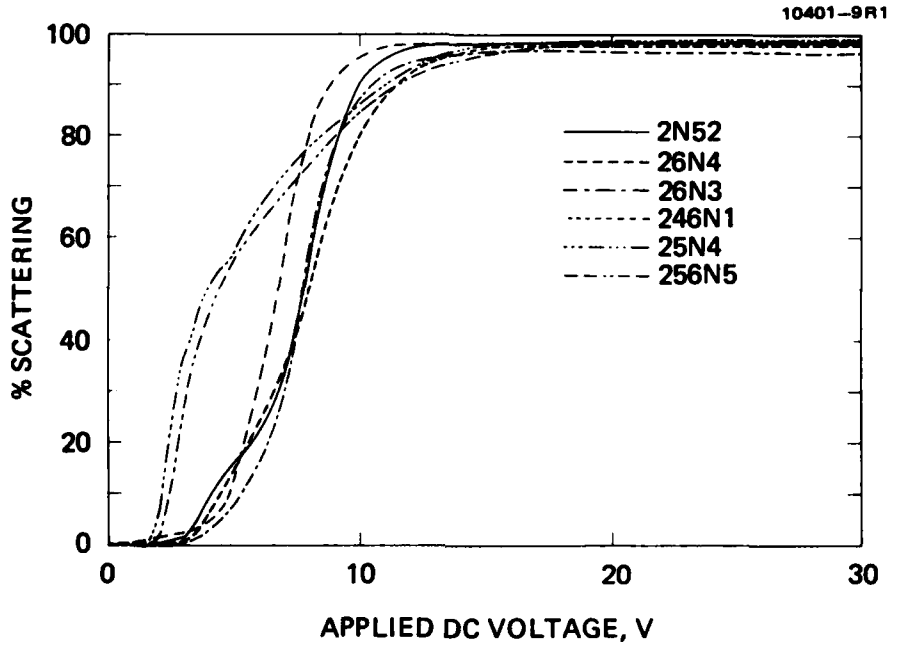

Figure 3. DS curves of redox-doped mixtures. (Transmission cells, 8.4 μm thick, surface-∥, 23°C, 0.5% DBF/TFM).

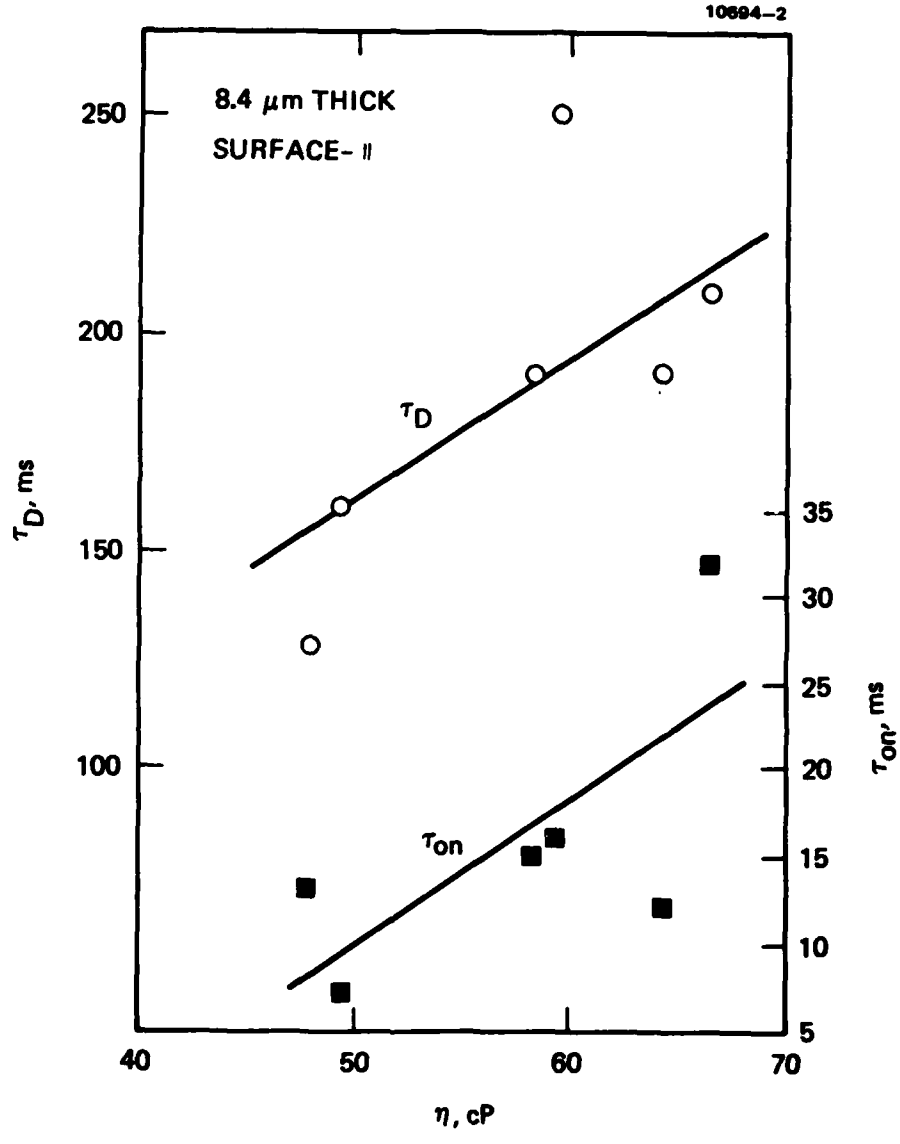

Figure 4. Viscosity effect on response times. (20 Vdc, 0.5% DBF/TFM, 25°C, τ_D = decay time from 100 to 10% S, τ_{ON} = time from 0 to 90% S.)

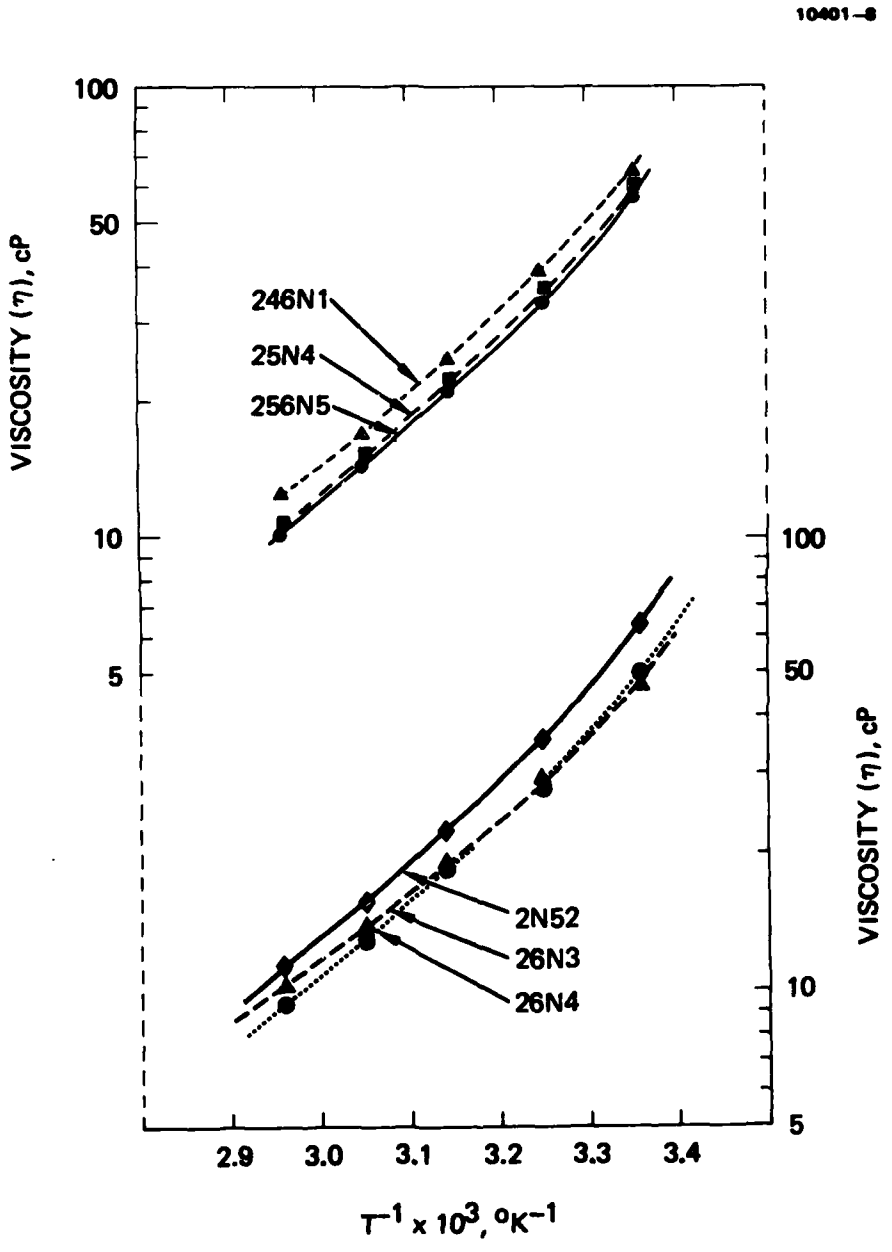

Figure 5. Flow viscosity of undoped mixtures.

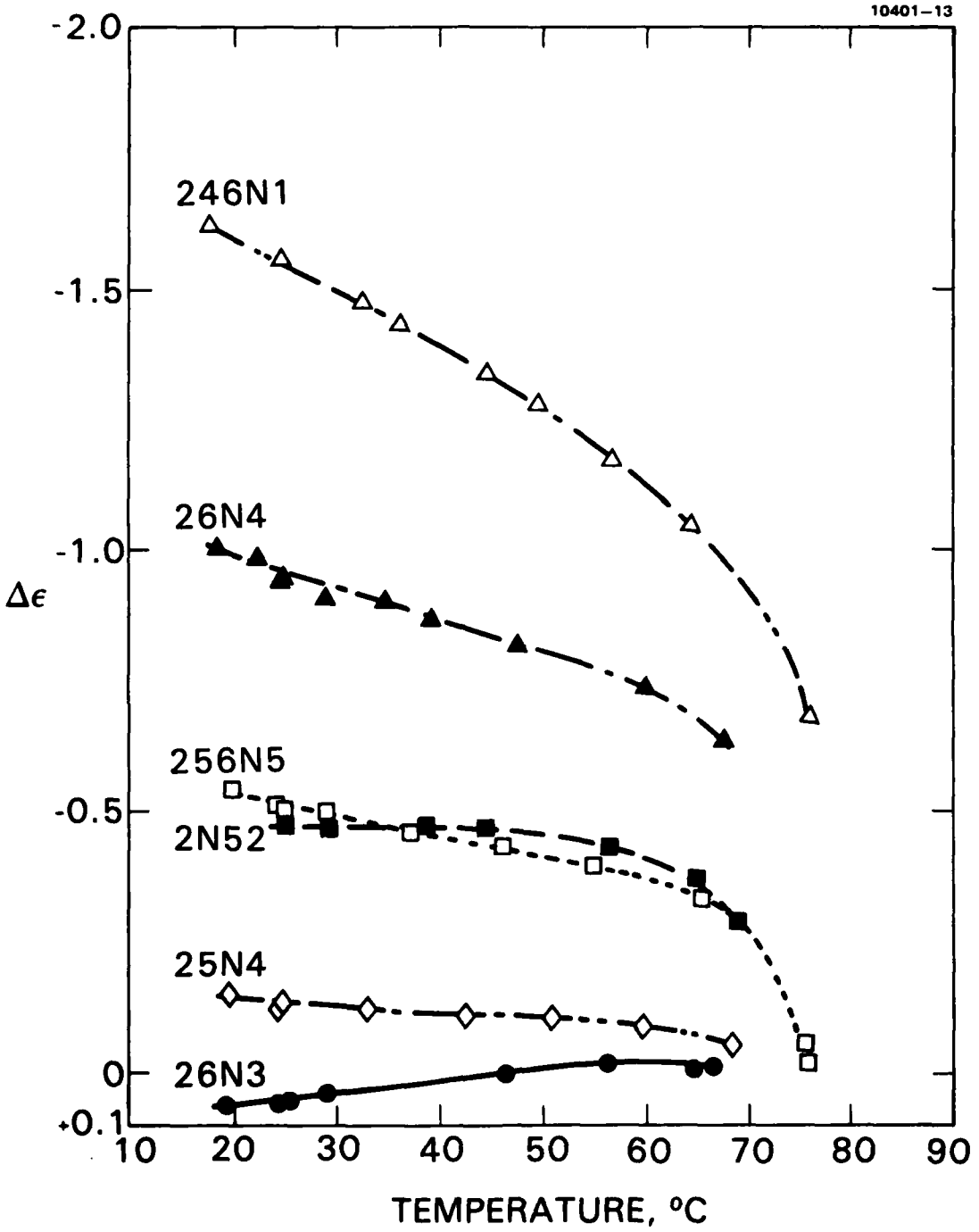

Figure 6. Effect of temperature on dielectric anisotropy of redox-doped mixtures (0.5% DBF/TFM).

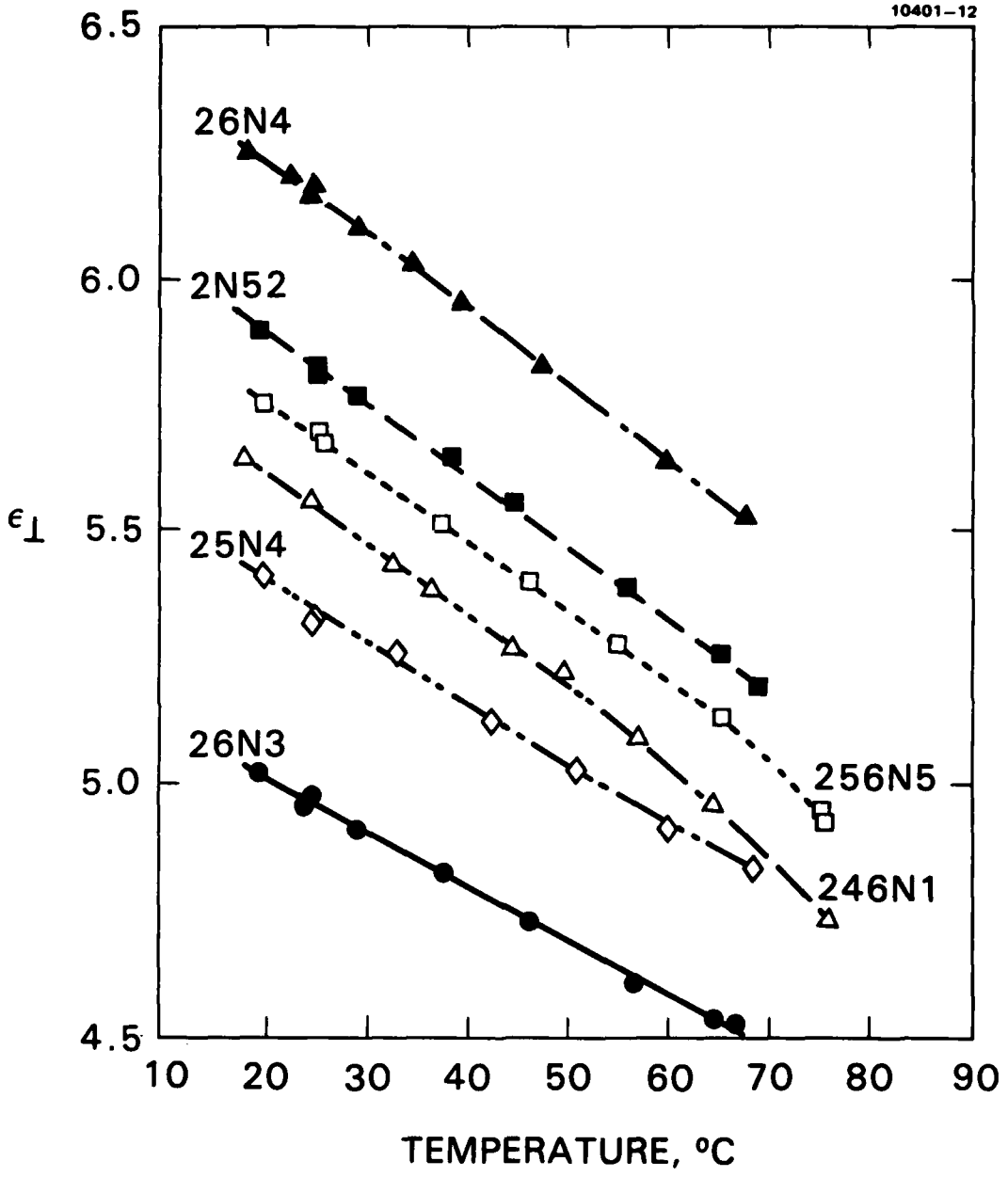

Figure 7. Effect of temperature on the $\varepsilon_\perp$ dielectric constant of redox-doped mixtures (0.5% DBF/TFM).

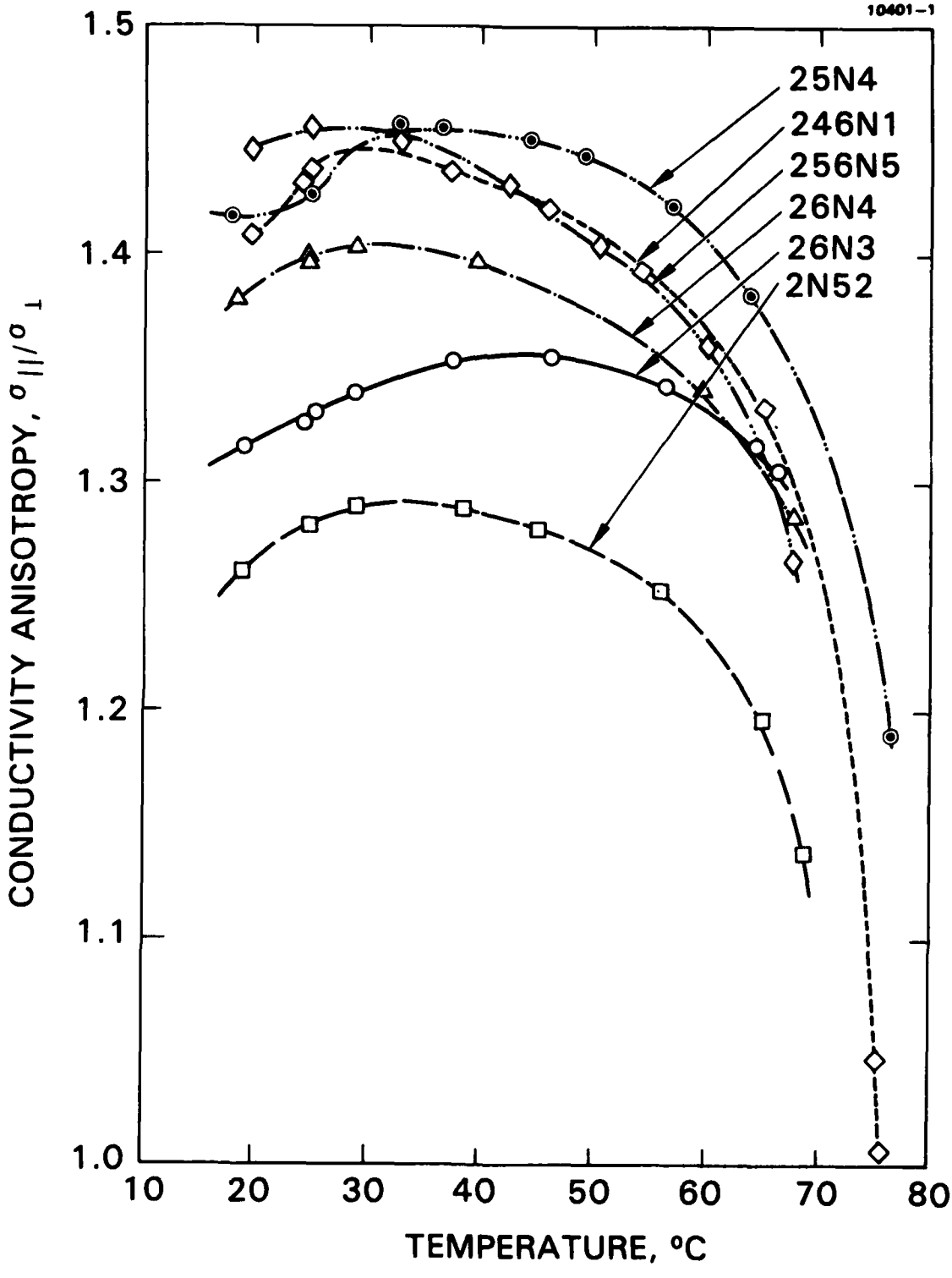

Figure 8. Effect of temperature on the $\sigma_{\parallel}/\sigma_{\perp}$ of redox-doped mixtures (0.5% DBF/TFM).

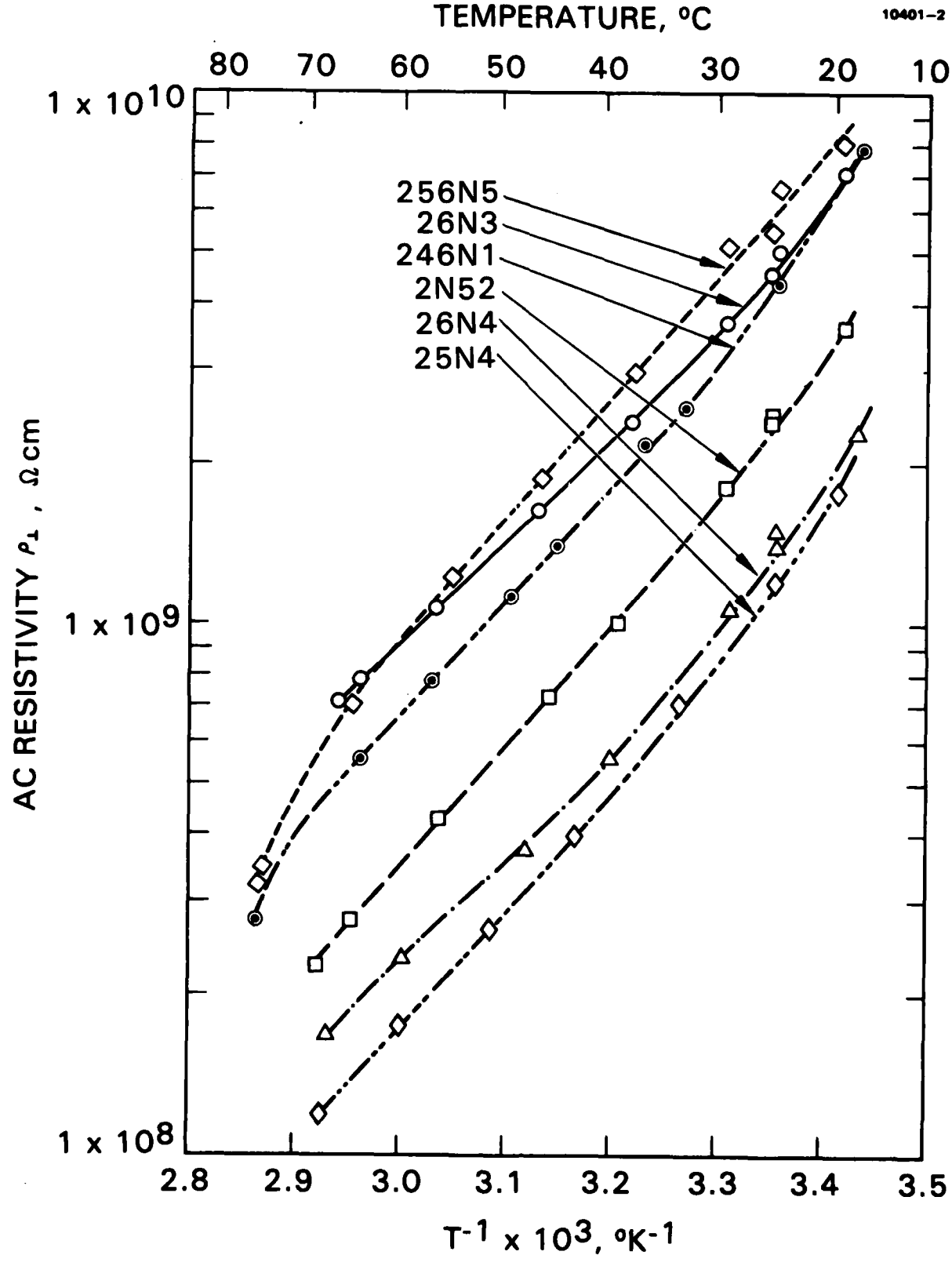

Figure 9. Effect of temperature on resistivity of redox-doped mixtures (0.5% DBF/TFM).

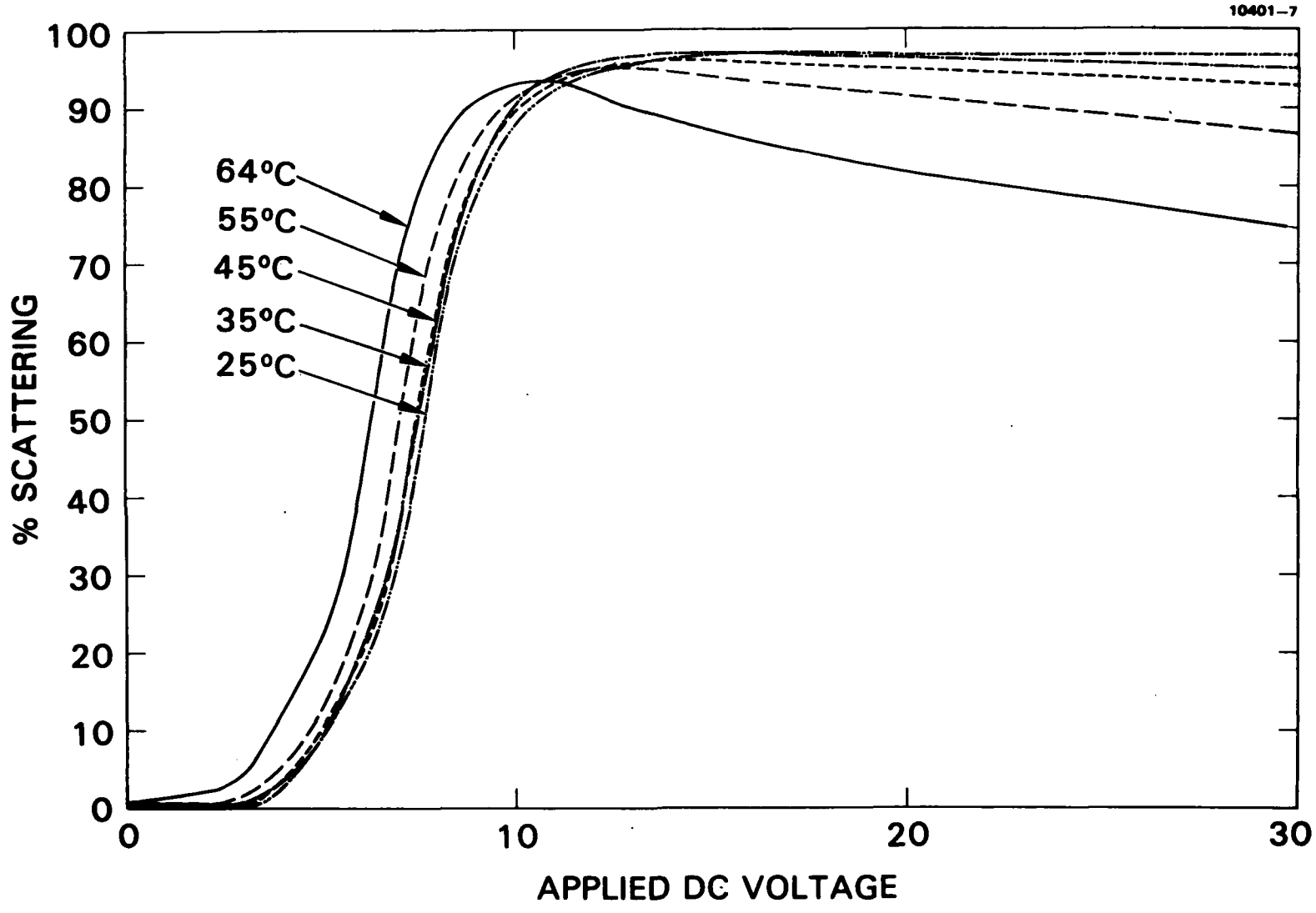

Figure 10. Temperature effect on dc-DS curves of redox-doped HRL-26N3. (Surface-Ⅱ, 8.4 μm thick, 0.5% DBF/TFM.)

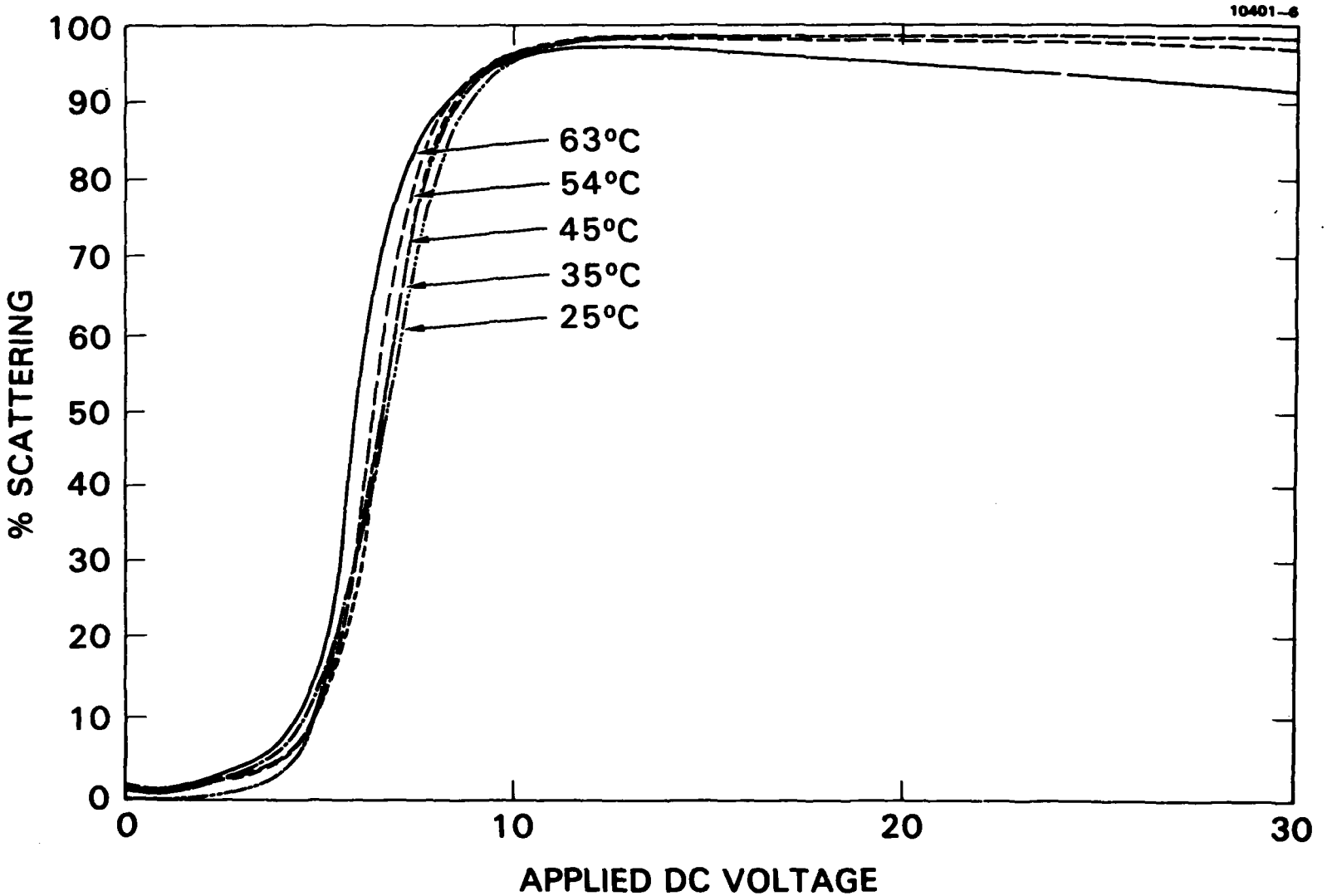

Figure 11. Temperature effect on DS curves of redox-doped HRL-26N4. (Surface-N, 8.4 μm thick, 0.5% DBF/TFM.)

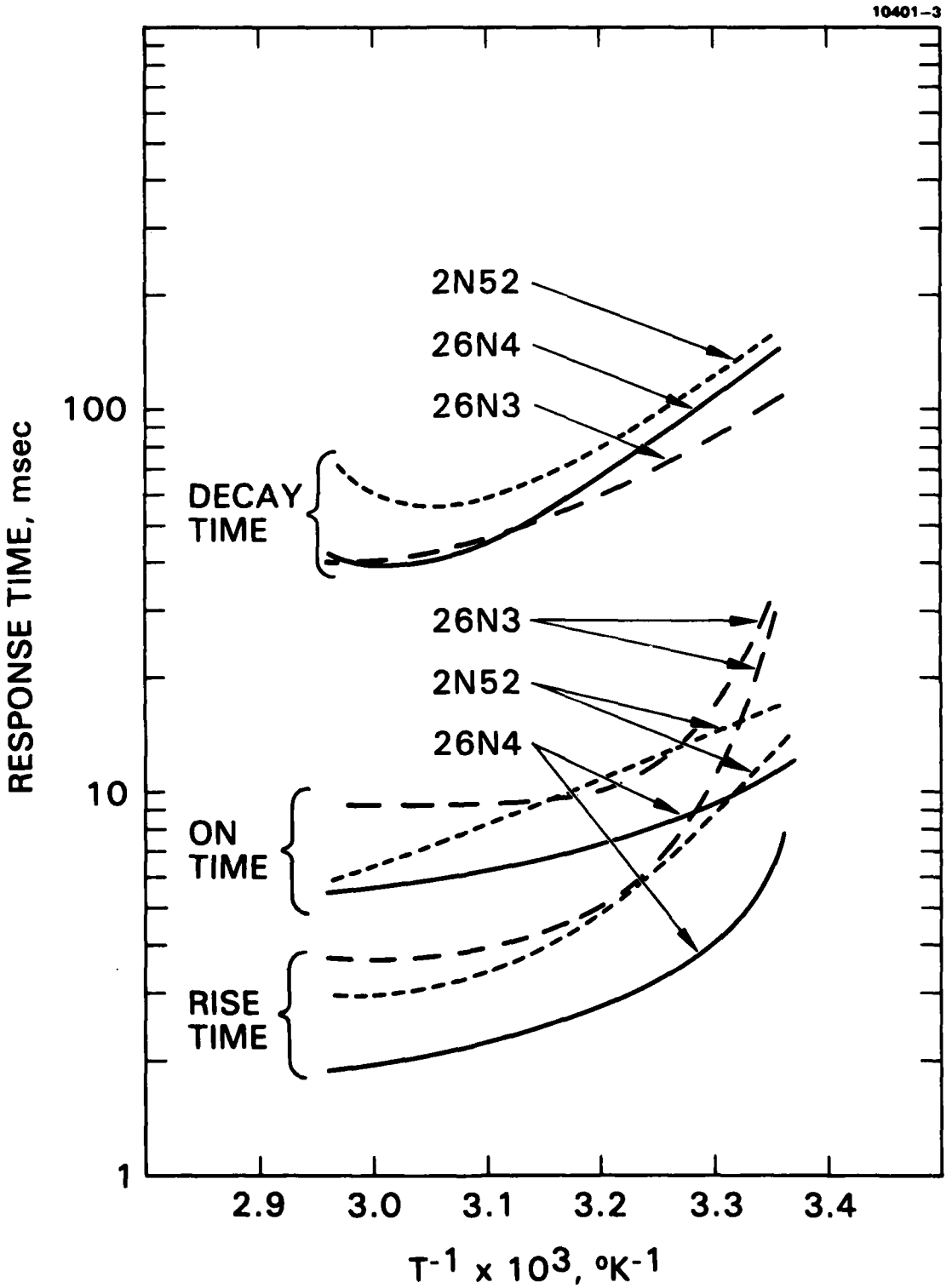

Figure 12. Effect of temperature on dc-DS response times from 15 V dc. (0.5% DBF/TFM, 8.4 μm thick, surface-Ⅱ.)

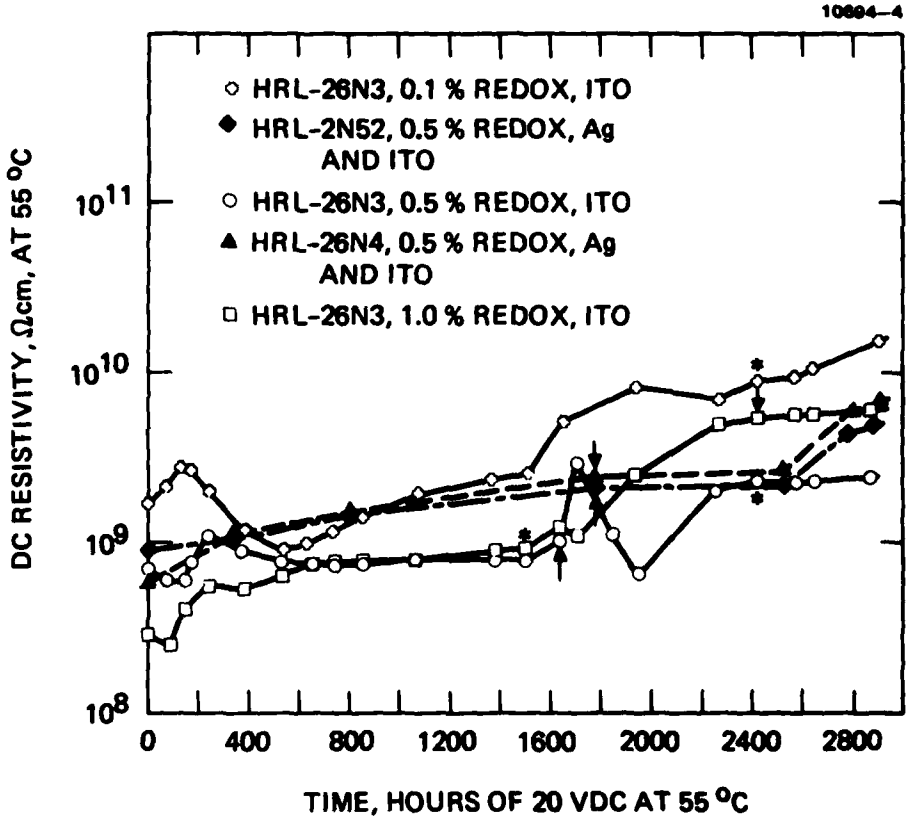

Figure 13. Electrochemical stability of DS at 55°C. (Unsealed cells, N_2, 13 μm thick, surface-‖, PVA coated except 26N3 with 0.5% redox. The * indicates crystals at 23°C; the ↓ is brown spots or ppt.)